Supplementary information for: A rapid application emissions-to-impacts tool for scenario assessment: Probabilistic Regional Impacts from Model patterns and Emissions (PRIME)

Camilla Mathison[1,3], Eleanor J. Burke[1], Eszter Kovacs[3], Gregory Munday[1], Chris Huntingford[2], Chris D. Jones[1,7], Chris J Smith[3,4], Norman J. Steinert[5], Andy J Wiltshire[1,6], Laila K. Gohar[1], and Rebecca M. Varney[6]

[1]Met Office Hadley Centre, Exeter, UK
[2]UK Centre for Ecology and Hydrology, Wallingford, UK
[3]University of Leeds, Leeds, UK
[4]International Institute for Applied Systems Analysis (IIASA), Laxenburg, Austria
[5]NORCE Norwegian Research Centre, Bjerknes Centre for Climate Research, Bergen, Norway
[6]Faculty of Environment, Science and Economy, University of Exeter, Exeter, UK
[7]School of Geographical Sciences, University of Bristol, Bristol, UK

1 Introduction

This is the supplementary information to accompany the paper: 'A rapid application emissions-to-impacts tool for scenario assessment: Probabilistic Regional Impacts from Model patterns and Emissions (PRIME)'.
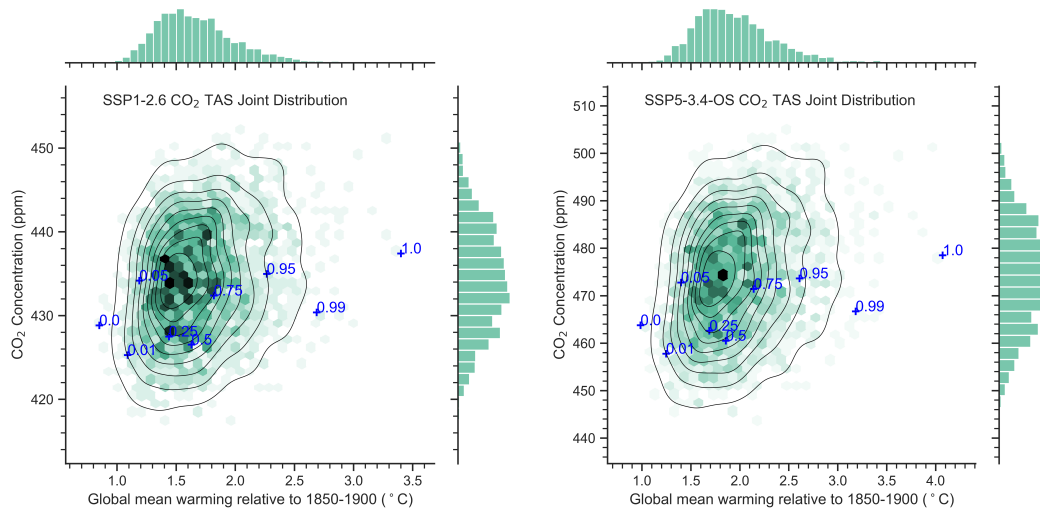
Figure S1. Joint distribution of Temperature (TAS) and CO_2 for SSP1-2.6 (left) and SSP5-3.4-OS (right) and the sub-selected percentiles (blue crosses) used to drive the JULES impacts model. Shades of green denote the density of points with individual histograms shown above and to the right of the main panel. 10% confidence intervals are shown by the contours.

## 2 Ensemble selection from temperature and CO_2 distribution

3 Evaluation of the patterns
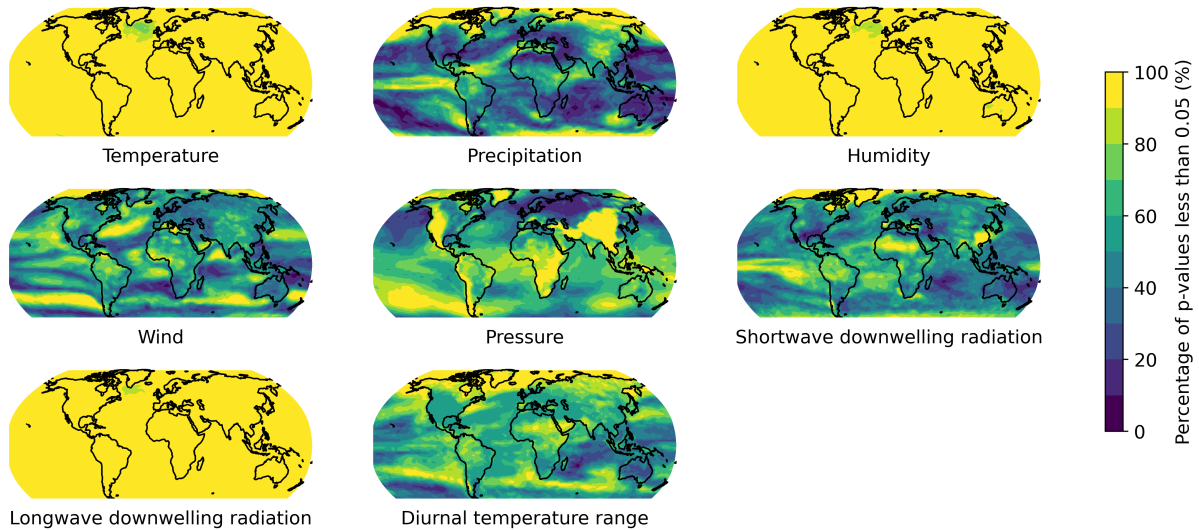
**Figure S2.** The percentage of the p-value for each JULES input variable (labelled) averaged over model and month for each pattern variable.
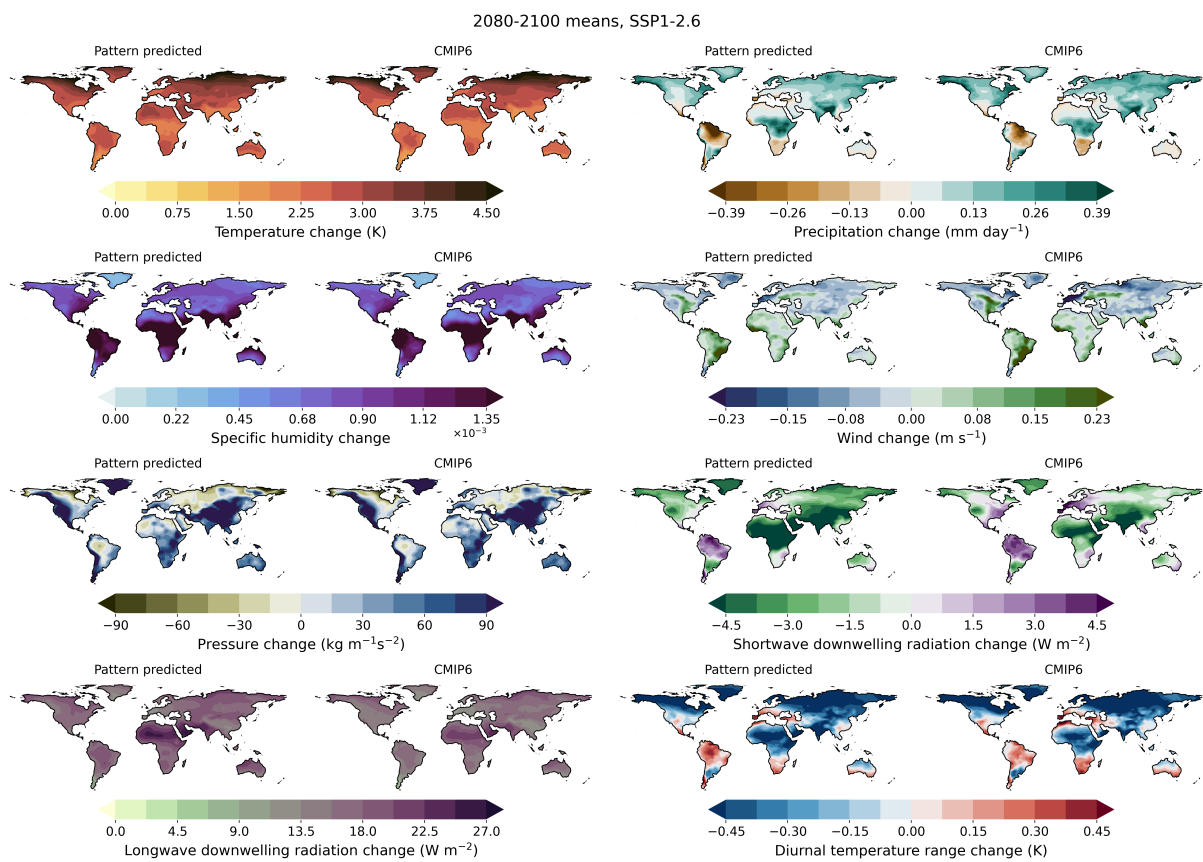
Figure S3. End of century changes (2080–2100) in each JULES input variable (labelled) for SSP1-2.6 predicted by patterns (left hand side of each variable panel) compared to CMIP6 values (right hand side of each variable panel). Plots shows the multi-model means.
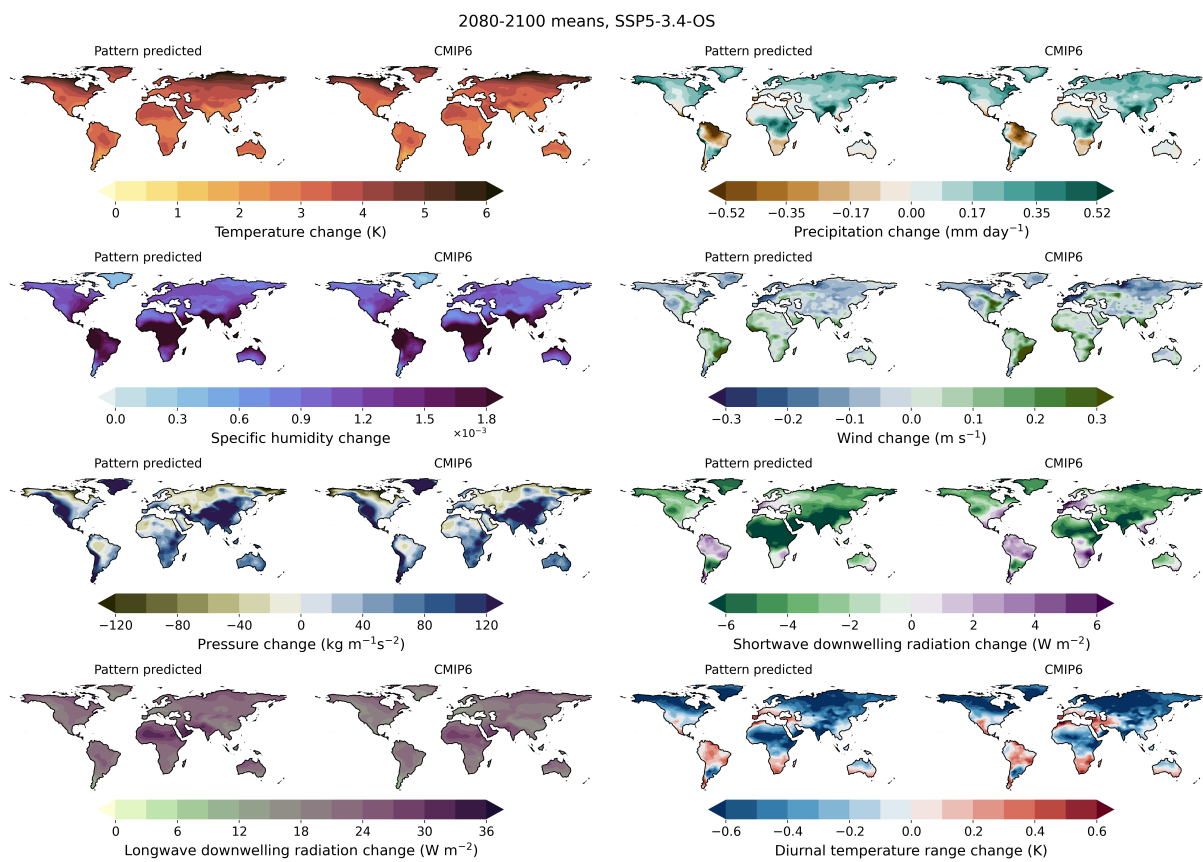
Figure S4. End of century changes (2080–2100) in each JULES input variable (labelled) for SSP5-3.4-OS predicted by patterns (left hand side of each variable panel) compared to CMIP6 values (right hand side of each variable panel). Plots shows the multi-model means.
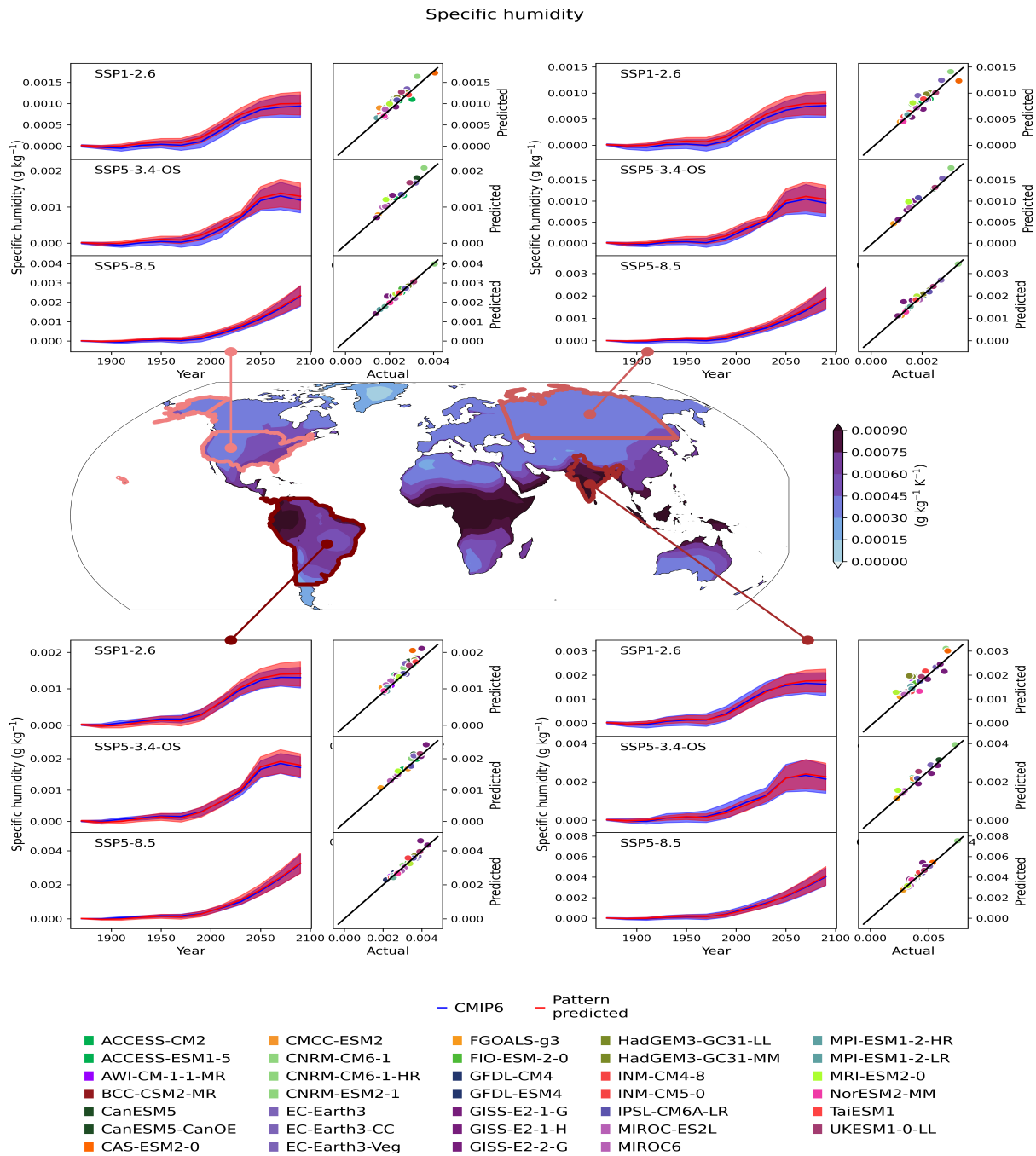
Specific humidity

Figure S5. The central map shows the specific humidity pattern (where there is no hatching indicates that the models tend to agree on the sign of the change and with hatching to show where the models tend to disagree on the sign of the change), and subpanels for each region: North America, Siberia, South America and South Asia. The region subpanels show the specific humidity timeseries (left subpanel) and scatter plots (right subpanel) for each scenario; top: SSP1-2.6, middle: SSP5-3.4-OS and bottom: S5P-8.5. The timeseries shows the PRIME patterns (blue plume) and the CMIP6 patterns (red plume). The scatter plots show the end of century values predicted by PRIME vs CMIP6 actual values for each model with the model colours shown at the bottom of the figure.
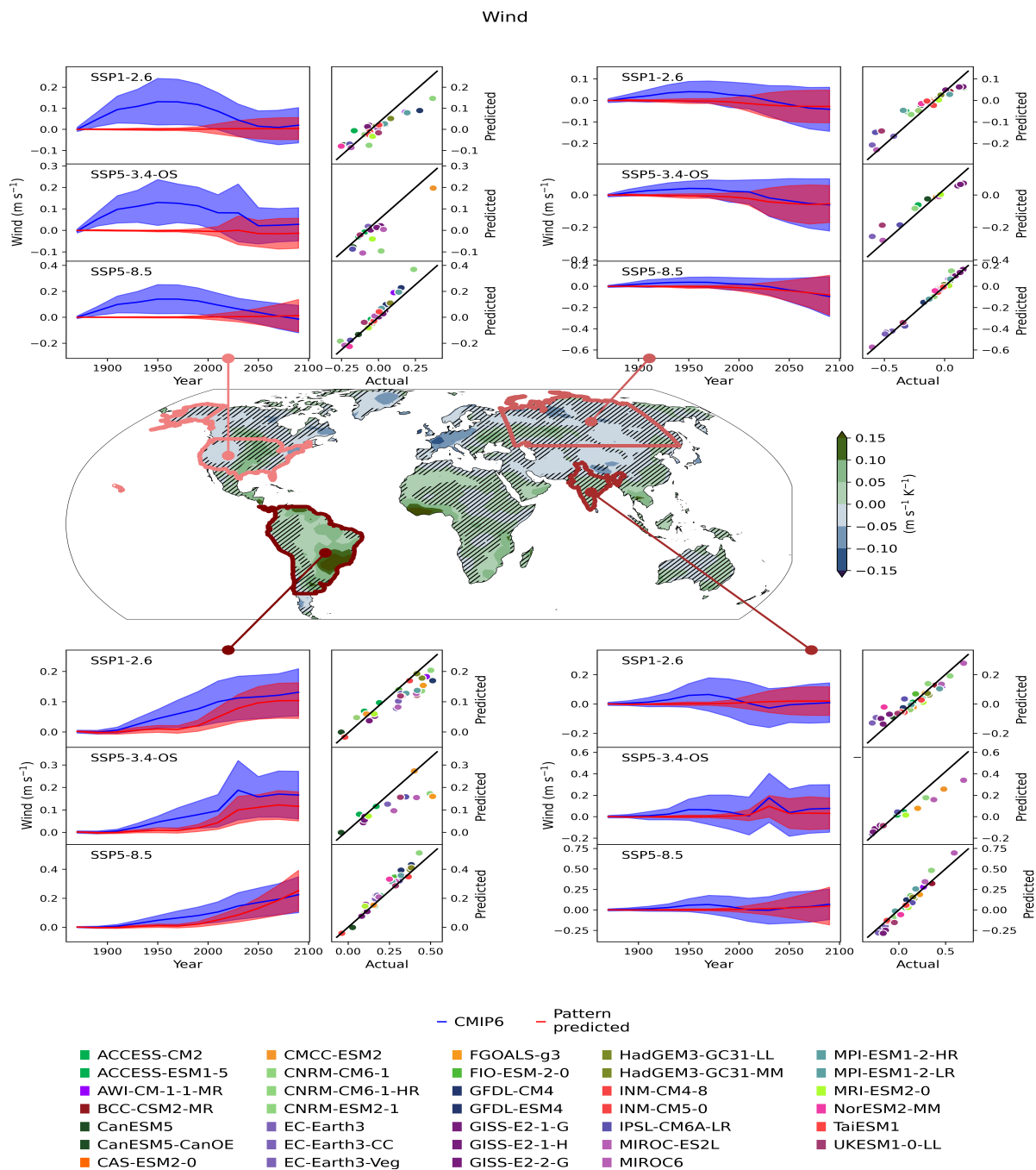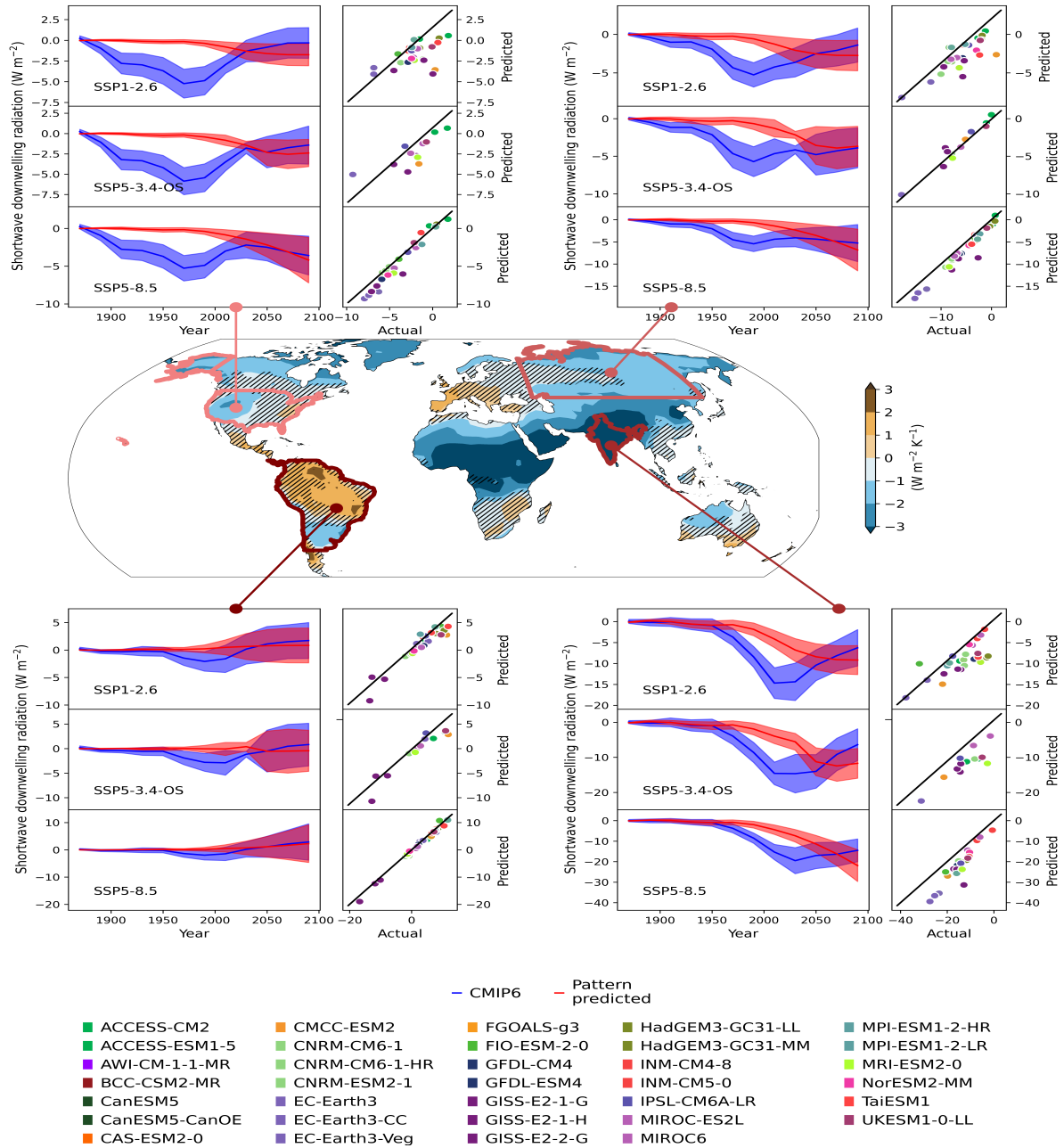
Figure S6. The central map shows the wind pattern (where there is no hatching indicates that the models tend to agree on the sign of the change and with hatching to show where the models tend to disagree on the sign of the change) and subpanels for each region: North America, Siberia, South America and South Asia. The region subpanels show the wind timeseries (left subpanel) and scatter plots (right subpanel) for each scenario; top: SSP1-2.6, middle: SSP5-3.4-OS and bottom: SSP5-8.5. The timeseries shows the PRIME patterns (blue plume) and the CMIP6 patterns (red plume). The scatter plots show the end of century values predicted by PRIME vs CMIP6 actual values for each model with the model colours shown at the bottom of the figure.
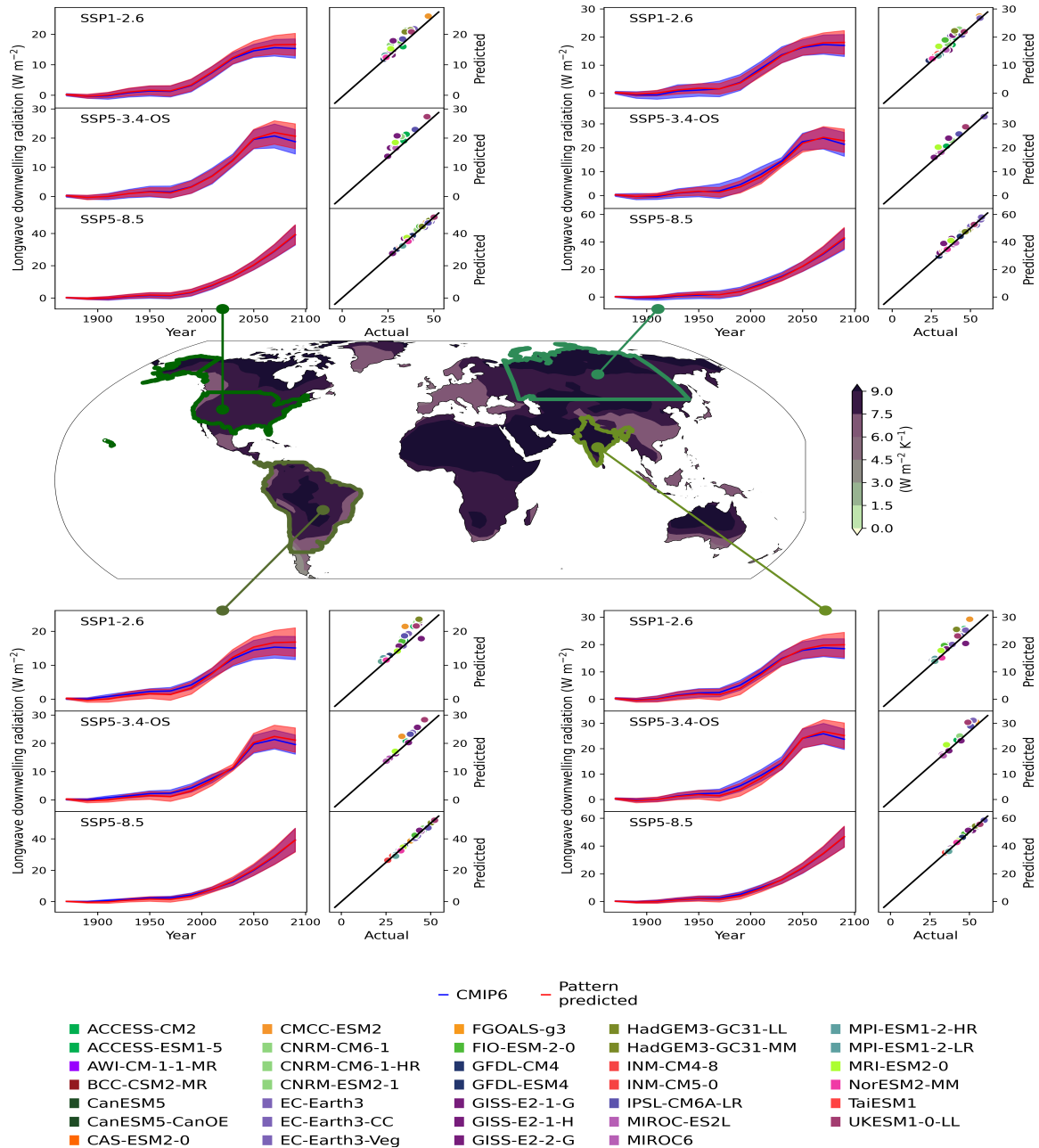
6
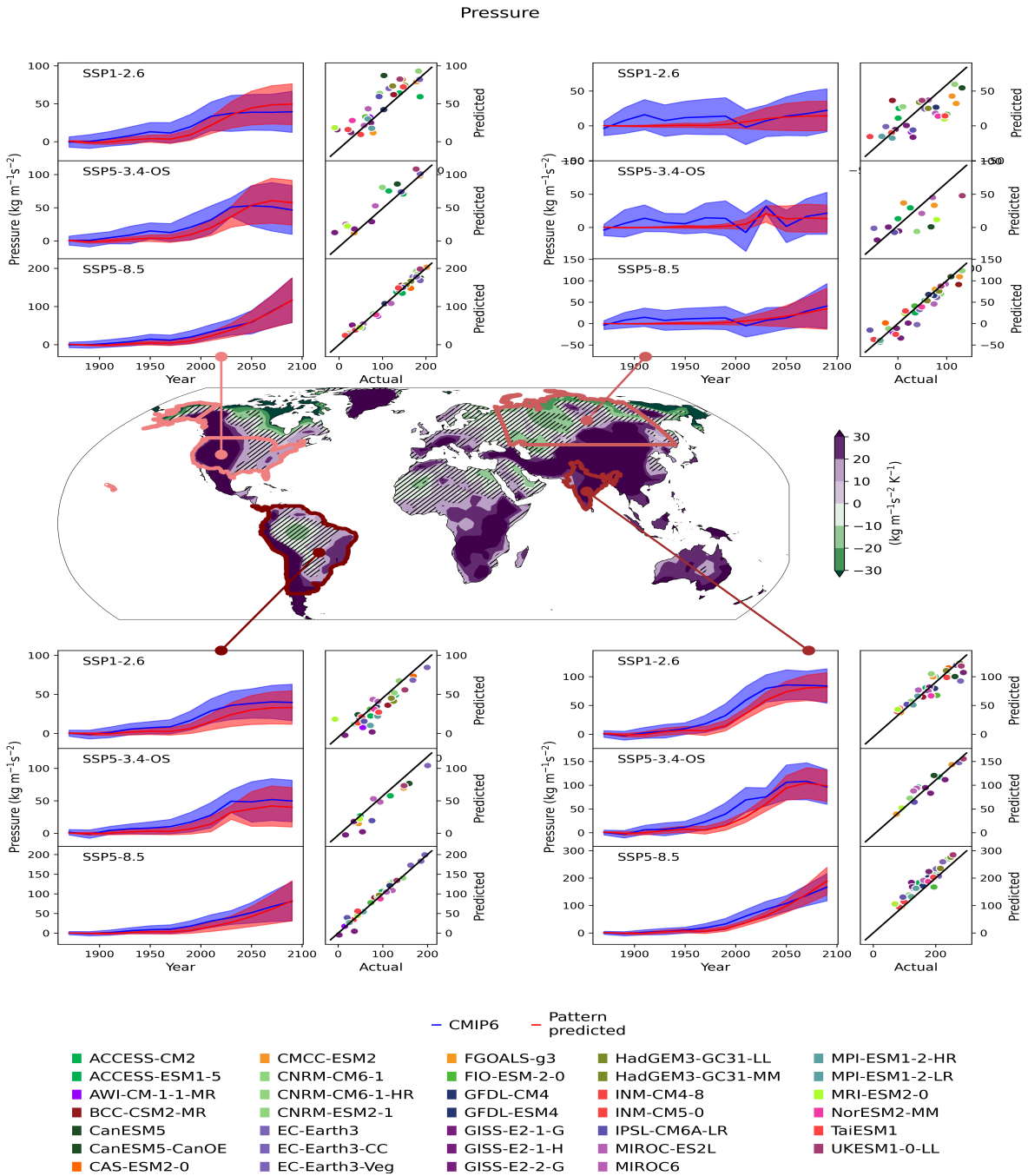
Figure S7. The central map shows the pressure pattern (where there is no hatching indicates that the models tend to agree on the sign of the change and with hatching to show where the models tend to disagree on the sign of the change) and subpanels for each region: North America, Siberia, South America and South Asia. The region subpanels show the pressure timeseries (left subpanel) and scatter plots (right subpanel) for each scenario; top: SSP1-2.6, middle: SSP5-3.4-OS and bottom: SSP5-8.5. The timeseries shows the PRIME patterns (blue plume) and the CMIP6 patterns (red plume). The scatter plots show the end of century values predicted by PRIME vs CMIP6 actual values for each model with the model colours shown at the bottom of the figure.

Shortwave downwelling radiation

Figure S8. The central map shows the shortwave downward radiation pattern (where there is no hatching indicates that the models tend to agree on the sign of the change and with hatching to show where the models tend to disagree on the sign of the change) and subpanels for each region: North America, Siberia, South America and South Asia. The region subpanels show the shortwave downward radiation timeseries (left subpanel) and scatter plots (right subpanel) for each scenario; top: SSP1-2.6, middle: SSP5-3.4-OS and bottom: SSP5-8.5. The timeseries shows the PRIME patterns (blue plume) and the CMIP6 patterns (red plume). The scatter plots show the end of century values predicted by PRIME vs CMIP6 actual values for each model with the model colours shown at the bottom of the figure.
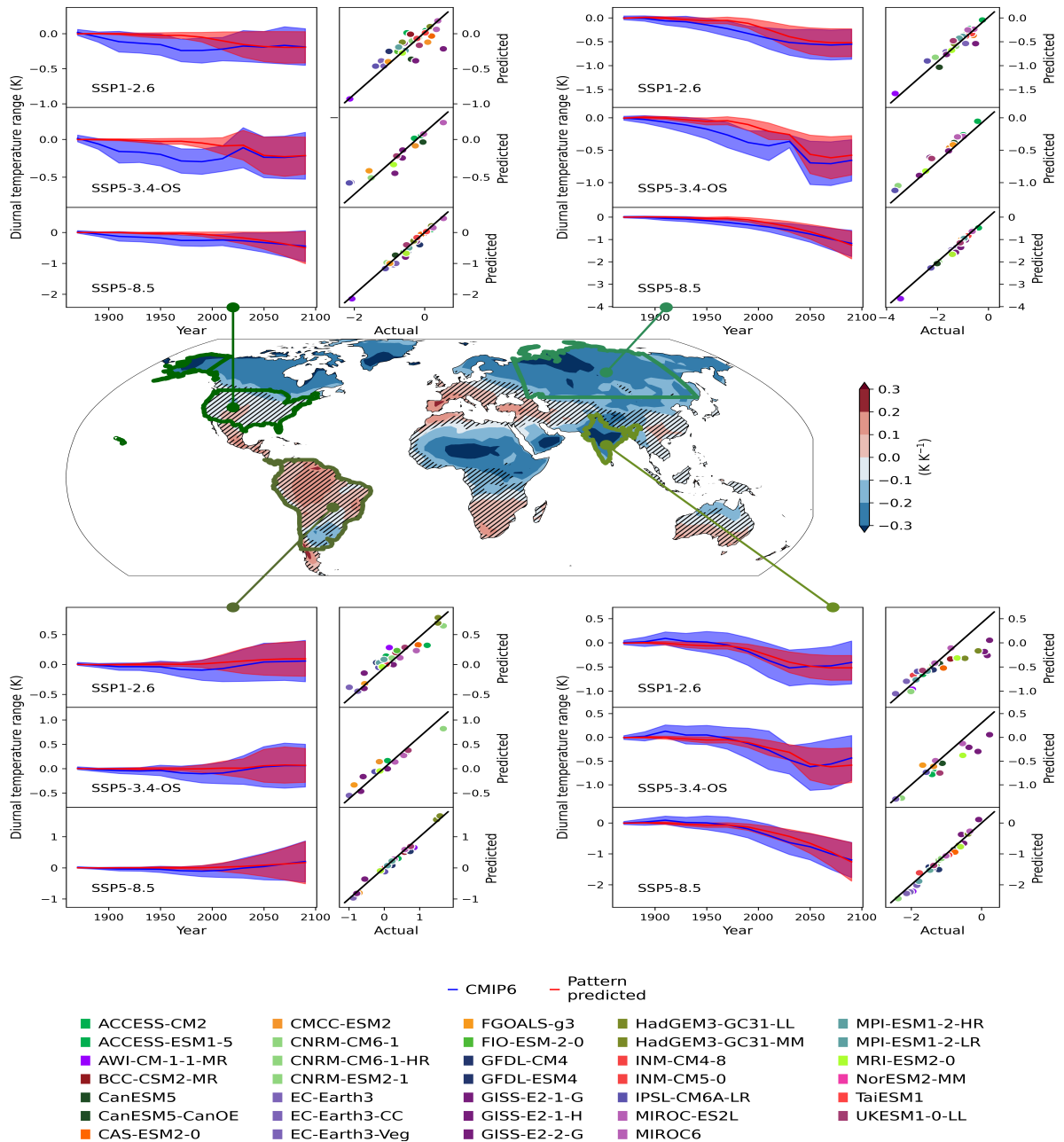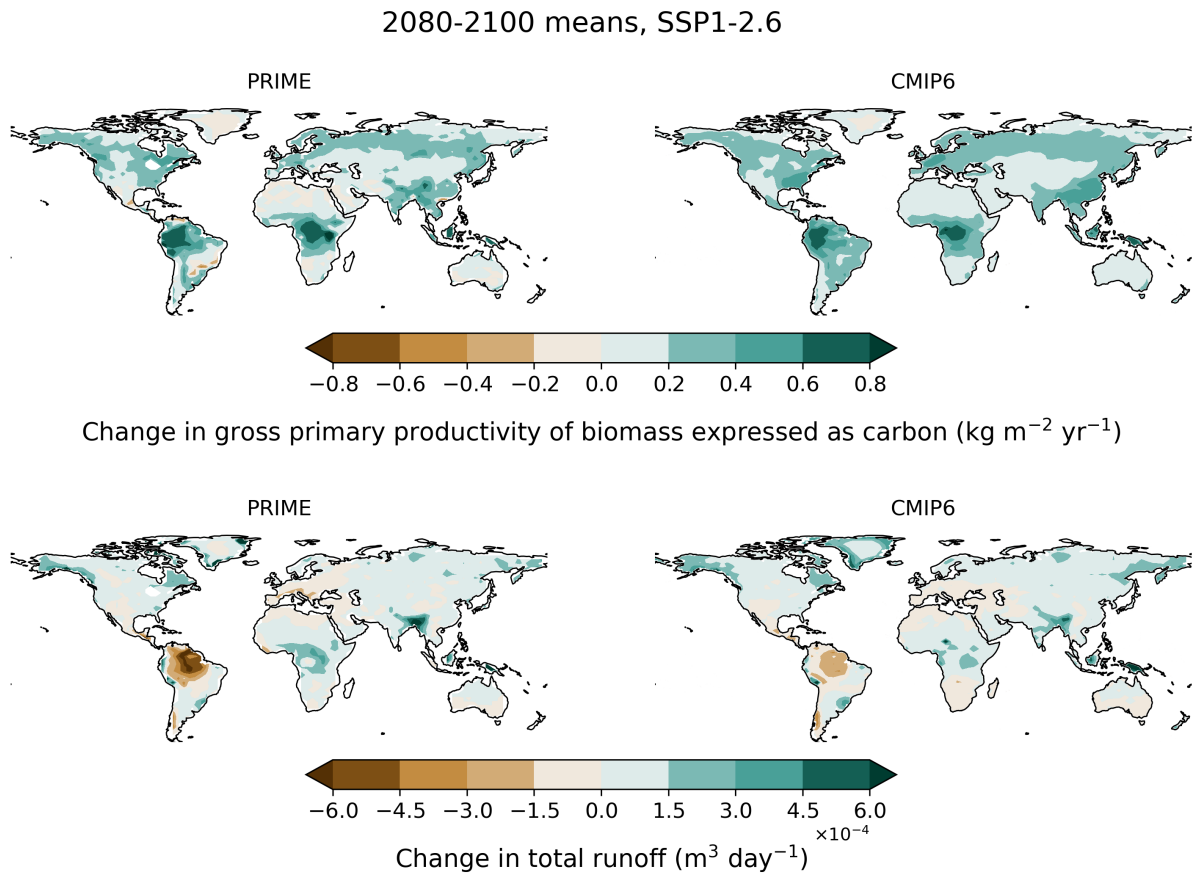
8

Longwave downwelling radiation

Figure S9. The central map shows the longwave downward radiation pattern (where there is no hatching indicates that the models tend to agree on the sign of the change and with hatching to show where the models tend to disagree on the sign of the change) and subpanels for each region: North America, Siberia, South America and South Asia. The region subpanels show the longwave downward radiation timeseries (left subpanel) and scatter plots (right subpanel) for each scenario; top: SSP1-2.6, middle: SSP5-3.4-OS and bottom: SSP5-8.5. The timeseries shows the PRIME patterns (blue plume) and the CMIP6 patterns (red plume). The scatter plots show the end of century values predicted by PRIME vs CMIP6 actual values for each model with the model colours shown at the bottom of the figure.
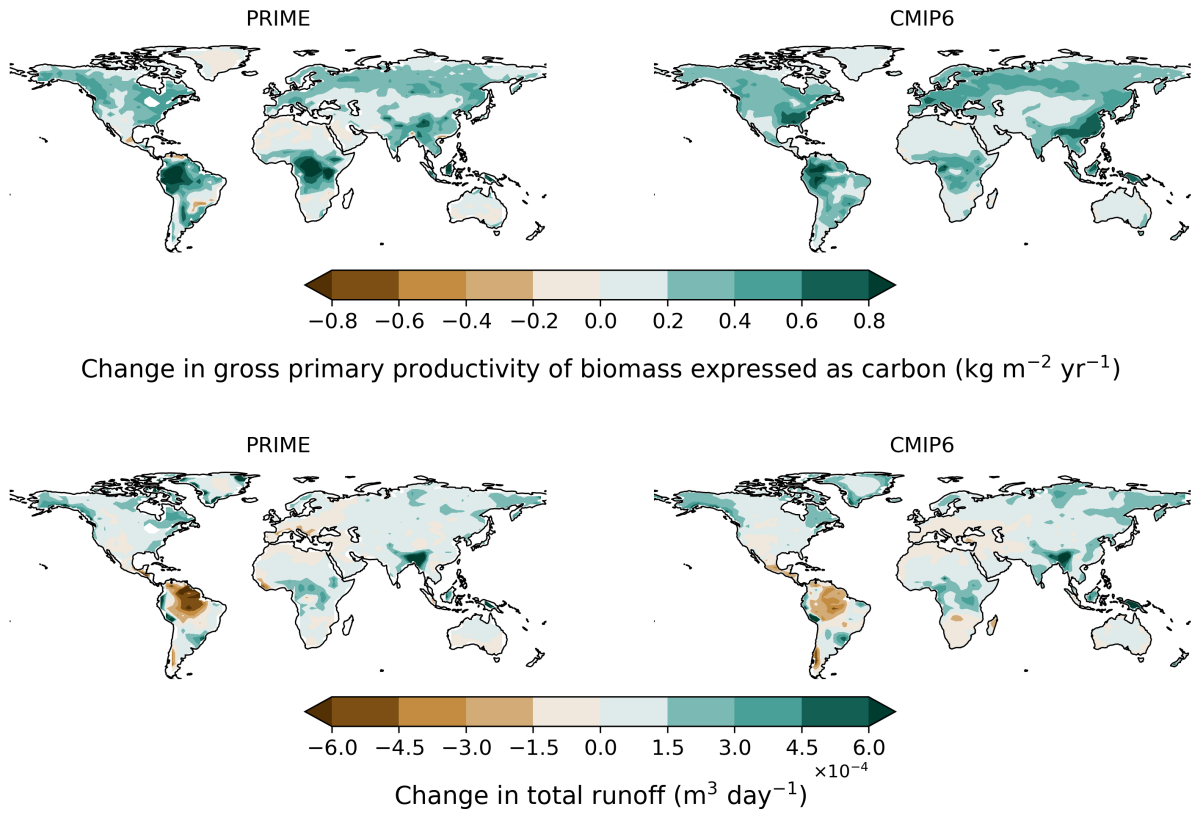
Diurnal temperature range

Figure S10. The central map shows the diurnal surface temperature range pattern (where there is no hatching indicates that the models tend to agree on the sign of the change and with hatching to show where the models tend to disagree on the sign of the change) and subpanels for each region: North America, Siberia, South America and South Asia. The region subpanels show the diurnal surface temperature range timeseries (left subpanel) and scatter plots (right subpanel) for each scenario; top: SSP1-2.6, middle: SSP5-3.4-OS and bottom: SSP5-8.5. The timeseries shows the PRIME patterns (blue plume) and the CMIP6 patterns (red plume). The scatter plots show the end of century values predicted by PRIME vs CMIP6 actual values for each model with the model colours shown at the bottom of the figure.

4 Evaluation of the JULES outputs

2080-2100 means, SSP1-2.6

Change in gross primary productivity of biomass expressed as carbon (kg m^{-2} yr^{-1})

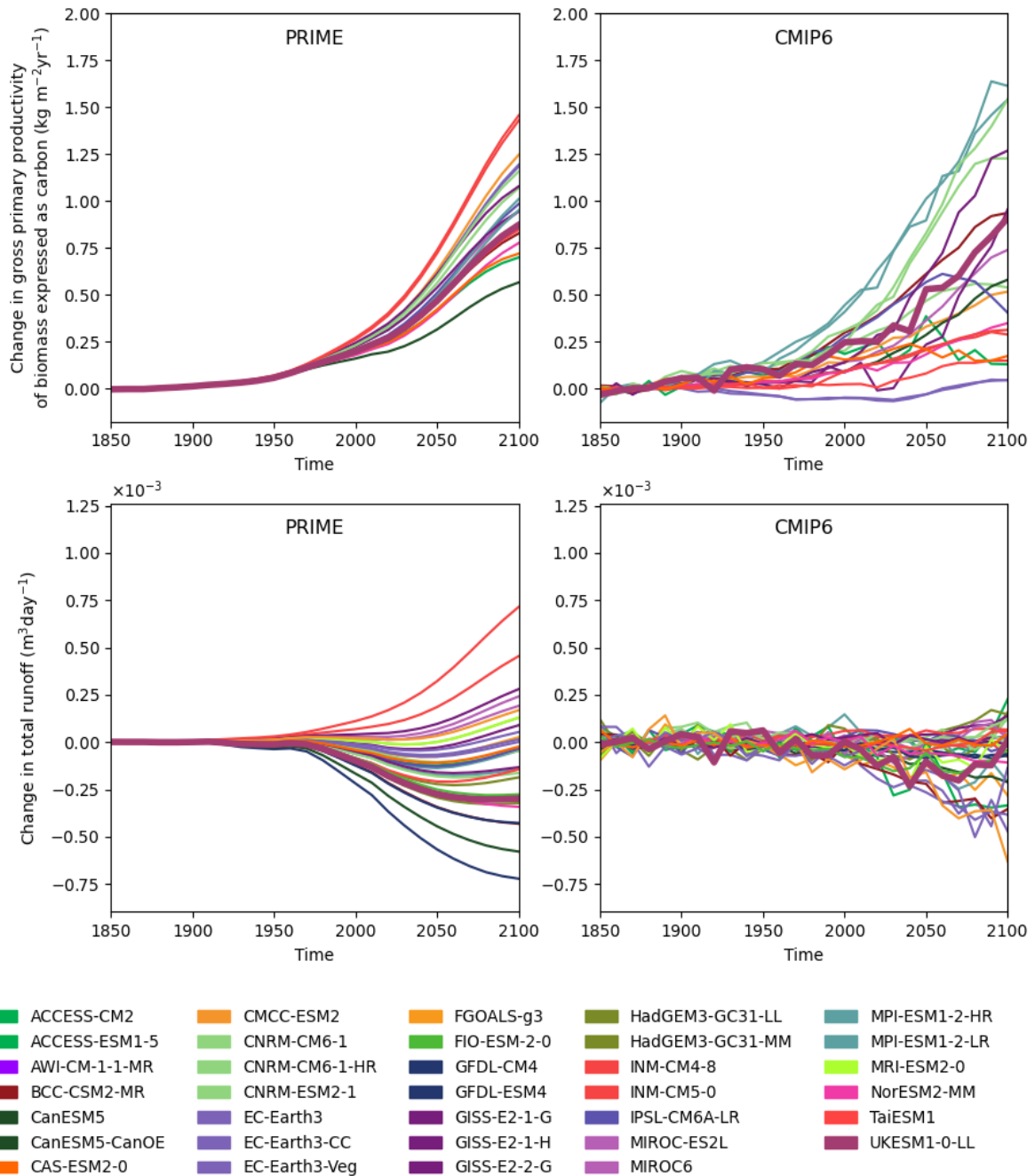Change in total runoff (m^3 day^{-1})

Figure S11. Maps comparing the multi-model mean projected end of century changes (2080–2100) for SSP1-2.6 for GPP (top) and runoff (bottom) from PRIME (left) compared to CMIP6 (right)

2080-2100 means, SSP5-3.4-OS

PRIME

CMIP6

Change in gross primary productivity of biomass expressed as carbon (kg m^{-2} yr^{-1})

PRIME

CMIP6

Change in total runoff (m^3 day^{-1})

Figure S12. Maps comparing the multi-model mean projected end of century changes (2080–2100) for SSP5-3.4-OS for GPP (top) and runoff (bottom) from PRIME (left) compared to CMIP6 (right)
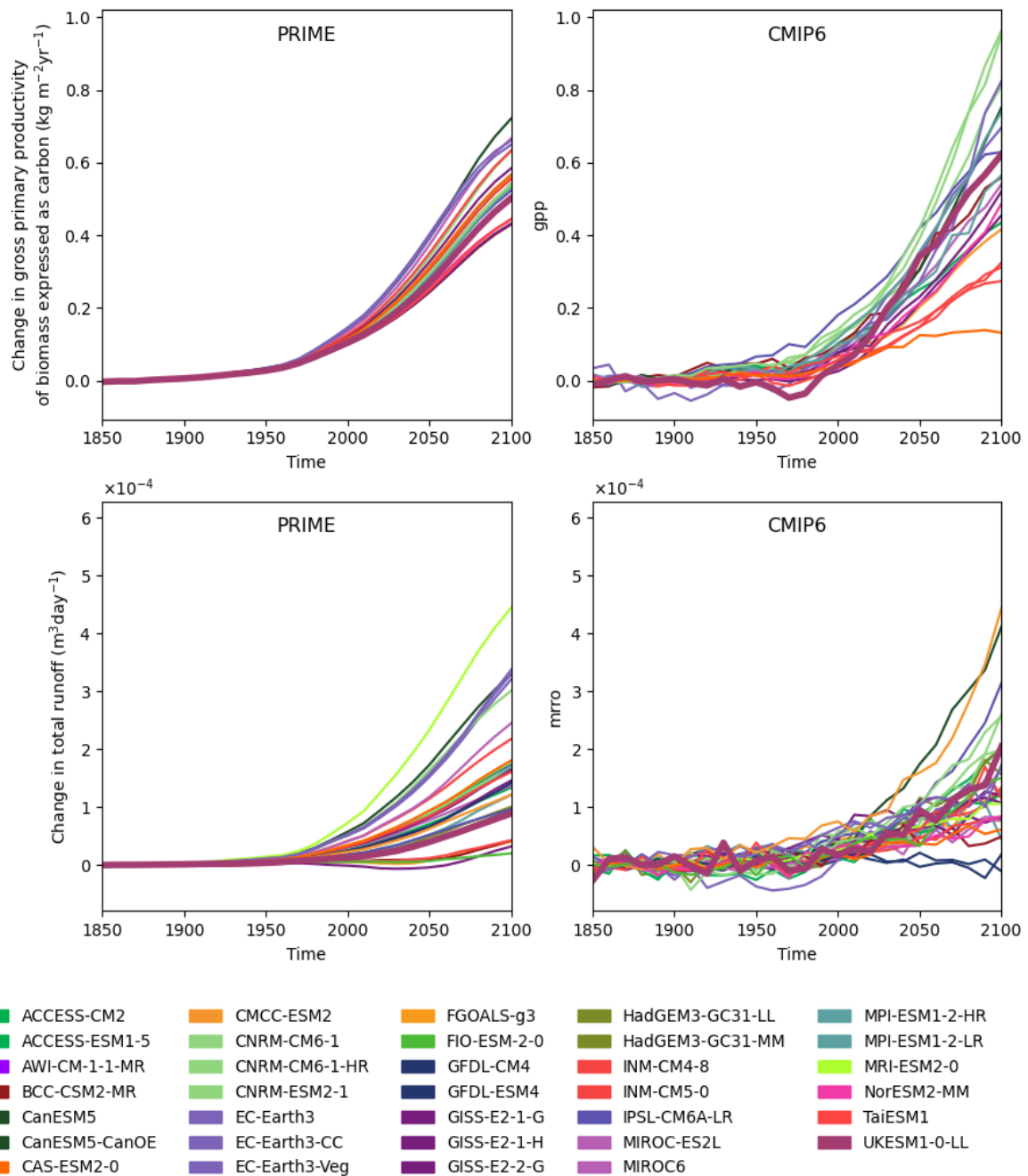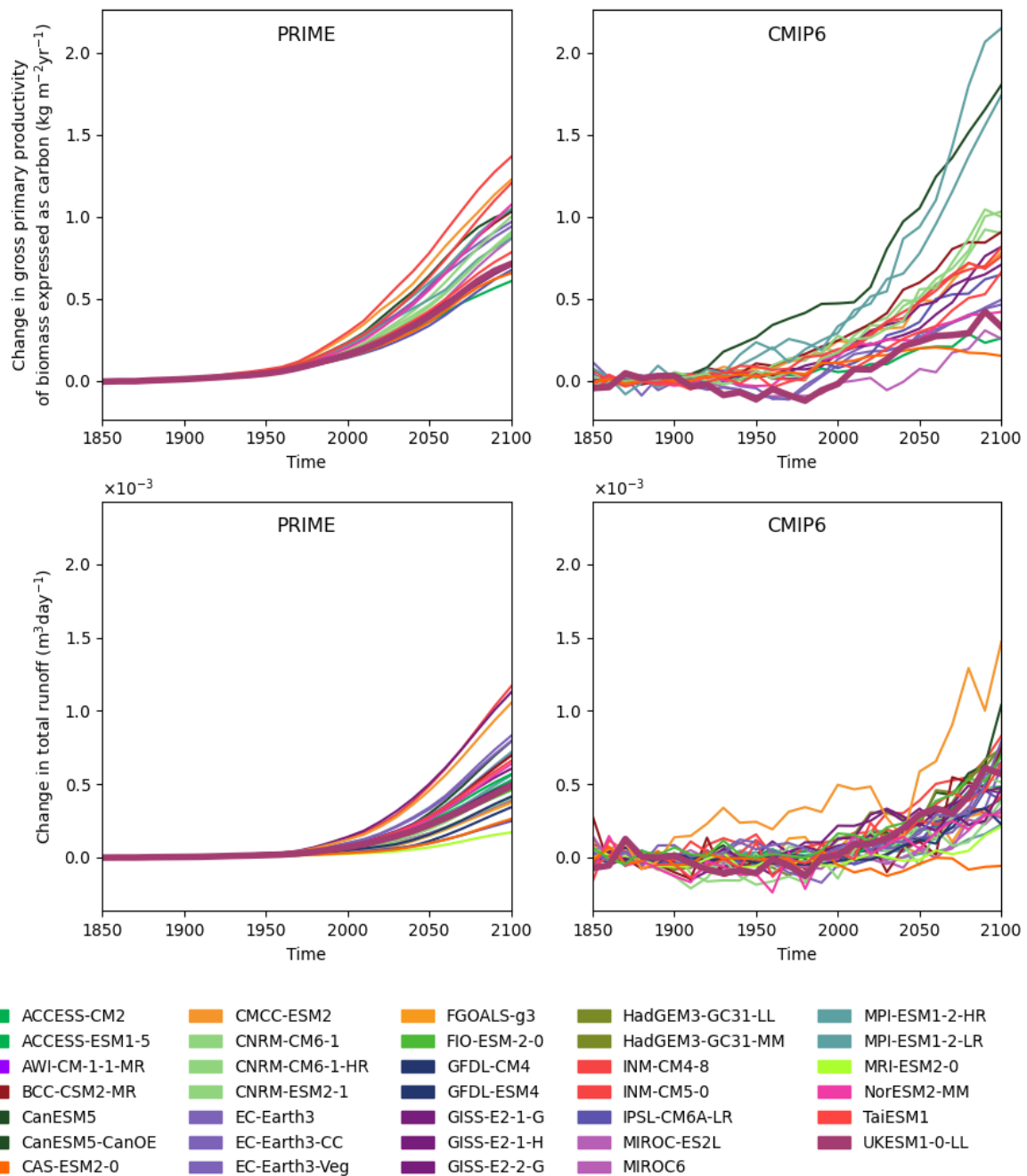
Figure S13. Timeseries of the change in gpp (top) and change in total runoff (bottom) for PRIME (left) and CMIP6 (right) for SSP5-8.5 for the Amazon region for each CMIP6 model

Figure S14. Timeseries of the change in gpp (top) and change in total runoff (bottom) for PRIME (left) and CMIP6 (right) for SSP5-8.5 for the Siberia region for each CMIP6 model

Figure S15. Timeseries of the change in gpp (top) and change in total runoff (bottom) for PRIME (left) and CMIP6 (right) for SSP5-8.5 for the India region for each CMIP6 model
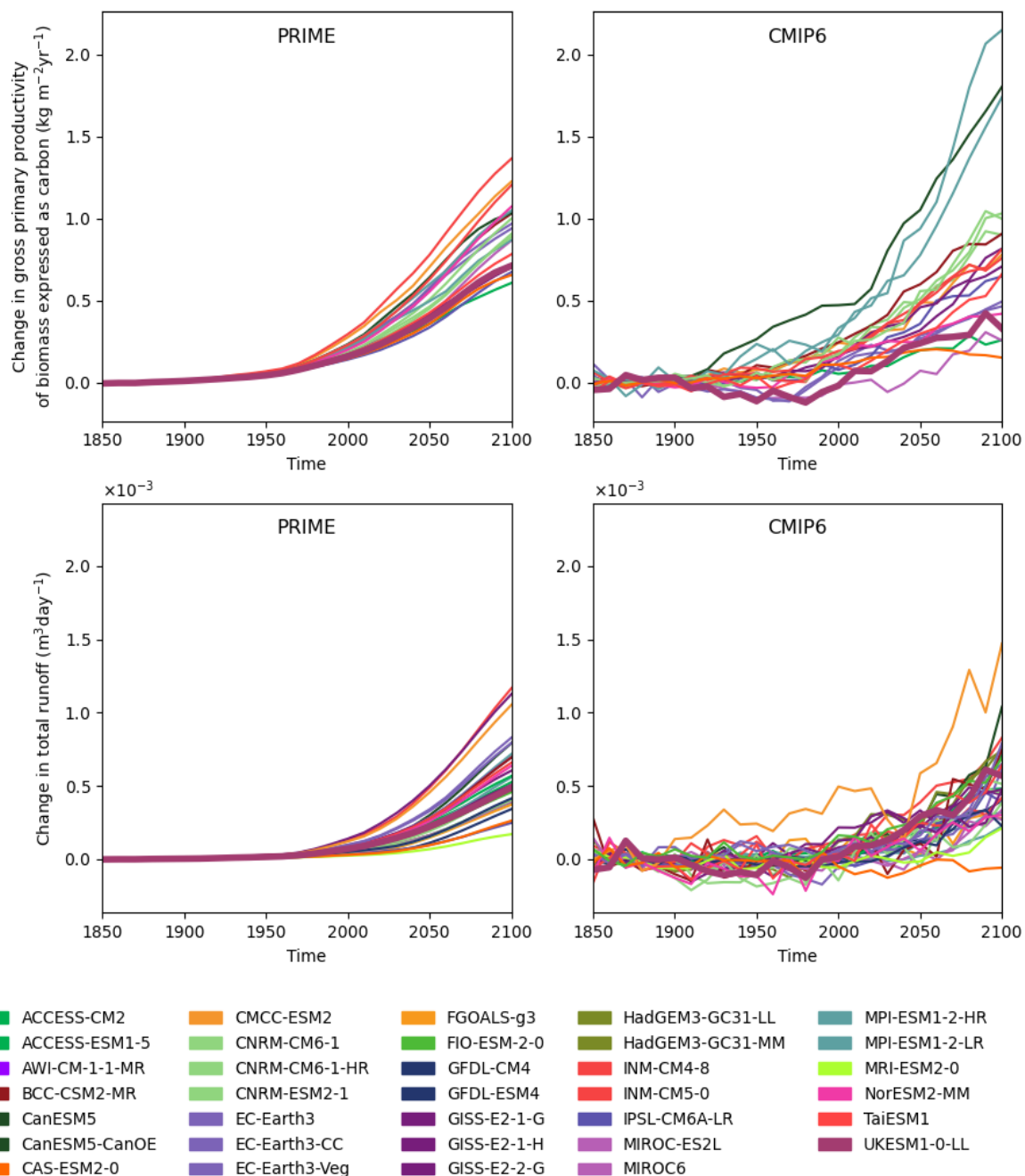
Figure S16. Timeseries of the change in gpp (top) and change in total runoff (bottom) for PRIME (left) and CMIP6 (right) for SSP5-8.5 for the USA region for each CMIP6 model

Table S1. SSP5-8.5 driven CMIP6 model patterns, selected based on data availability.

	Model	Realisation
1.	ACCESS-CM2	r1i1p1f1
2.	ACCESS-ESM1-5	r3i1p1f1
3.	AWI-CM-1-1-MR	r1i1p1f1
4.	BCC-CSM2-MR	r1i1p1f1
5.	CAS-ESM2-0	r1i1p1f1
6.	CMCC-ESM2	r1i1p1f1
7.	CNRM-CM6-1	r1i1p1f2
8.	CNRM-CM6-1-HR	r1i1p1f2
9.	CNRM-ESM2-1	r1i1p1f2
10.	CanESM5	r1i1p1f1
11.	CanESM5-CanOE	r1i1p2f1
12.	EC-Earth3	r11i1p1f1
13.	EC-Earth3-CC	r1i1p1f1
14.	EC-Earth3-Veg	r1i1p1f1
15.	FGOALS-g3	r1i1p1f1
16.	FIO-ESM-2-0	r1i1p1f1
17.	GFDL-CM4	r1i1p1f1
18.	GFDL-ESM4	r1i1p1f1
19.	GISS-E2-1-G	r1i1p5f1
20.	GISS-E2-1-H	r3i1p1f2
21.	GISS-E2-2-G	r1i1p3f1
22.	HadGEM3-GC31-LL	r1i1p1f3
23.	HadGEM3-GC31-MM	r1i1p1f3
24.	INM-CM4-8	r1i1p1f1
25.	INM-CM5-0	r1i1p1f1
26.	IPSL-CM6A-LR	r1i1p1f1
27.	MIROC-ES2L	r1i1p1f2
28.	MIROC6	r1i1p1f1
29.	MPI-ESM1-2-HR	r1i1p1f1
30.	MPI-ESM1-2-LR	r1i1p1f1
31.	MRI-ESM2-0	r1i1p1f1
32.	NorESM2-MM	r1i1p1f1
33.	TaiESM1	r1i1p1f1
34.	UKESM1-0-LL	r1i1p1f2